FOXA1 Is a Potential Oncogene in Anaplastic Thyroid Carcinoma

Carmelo Nucera,[1] Jerome Eeckhoute,[1] Stephen Finn,[2] Jason S. Carroll,[3] Azra H. Ligon,[2,10] Carmen Priolo,[4] Guido Fadda,[5] Mary Toner,[6] Orla Sheils,[7] Marco Attard,[8] Alfredo Pontecorvi,[9] Vânia Nose,[10] Massimo Loda,[2,4,10] and Myles Brown[1,11]

Abstract

Purpose: FOXA1 is a mammalian endodermal transcription factor belonging to the human forkhead box gene family that plays a role in certain tumor types. Here, we investigated the potential role of *FOXA1* in human thyroid carcinomas.

Experimental Design: We examined the level of FOXA1 expression and gene copy number by immunohistochemistry and fluorescence *in situ* hybridization, respectively, in a cohort of benign and malignant thyroid tumors. In addition, we examined the role of FOXA1 in the proliferation of an undifferentiated thyroid carcinoma cell line by short hairpin RNA-mediated silencing.

Results: We show that FOXA1 is overexpressed in human anaplastic thyroid carcinomas (ATC). In addition, we identify *FOXA1* DNA copy number gain within the 14q21.1 locus in both an ATC cell line and human ATC cases. Silencing of *FOXA1* in an ATC cell line causes G_1 growth arrest and reduction of cell proliferation. Moreover, we observe a potential link between FOXA1 and the cell cycle machinery by identifying $p27^{kip1}$ upregulation on *FOXA1* silencing.

Conclusions: *FOXA1* is overexpressed in aggressive thyroid cancers and involved in cell cycle progression in an ATC cell line. Therefore, *FOXA1* may be an important oncogene in thyroid tumorigenesis and a potential new therapeutic target for the treatment of anaplastic thyroid cancers.

Malignant tumors of thyroid follicular cells have been classified as either well-differentiated thyroid carcinomas, represented by papillary and follicular thyroid carcinomas, or undifferentiated (anaplastic) thyroid carcinoma (ATC). Although the majority of either well-differentiated thyroid carcinomas are indolent malignancies with a 10-year survival of up to 90% (1), ATC, which represents ~2% of all thyroid cancers, is one of the most aggressive malignancies known, rapidly invading the neck and often spreading to other organs (2). ATC is thought to develop from an existing papillary or follicular cancer and is responsible for more than half of thyroid carcinoma deaths, with a mean survival of 6 months from diagnosis (3). In fact, neither chemotherapy nor radiation therapy are effective to prolong ATC patient survival (4). Therefore, alternative systemic treatment for this cancer are urgently needed.

ATC have a very high proliferation rate and marked aneuploidy (5). Several genes involved in cell proliferation and cell cycle regulation have been shown to be dysregulated in these tumors (6). In addition, it has been recently reported that thyroid-specific transcription factors crucial for thyroid organogenesis and differentiation, such as Pax8, TTF-1, and TTF-2 (FOXE1), are expressed in thyroid neoplasms (7). In particular, Pax8 is highly expressed in ATC, whereas TTF-1 and FOXE1 were seen in a lower percentage (7).

FOXA factors are members of the winged helix/forkhead box family and play important roles during multiple phases of mammalian life, regulating development of endodermal primordia and organogenesis as well as regulating metabolism and homeostasis in the adult (8–10). In particular, *FOXA1* (hepatocyte nuclear factor 3α) is involved in hepatic differentiation and is an endodermal "pioneer transcription factor," binding to promoters and enhancers enabling chromatin access for other tissue-specific transcription factors (11, 12). This transcription

Authors' Affiliations: [1]Division of Molecular and Cellular Oncology, Department of Medical Oncology, Dana-Farber Cancer Institute and Harvard Medical School, Boston, Massachusetts; [2]Department of Medical Oncology, Center for Molecular Oncologic Pathology, Dana-Farber Cancer Institute, Harvard Medical School, Boston, Massachusetts; [3]Cancer Research UK, Cambridge Research Institute, Cambridge, United Kingdom; [4]Department of Medical Oncology, Dana-Farber Cancer Institute, Harvard Medical School, Boston; [5]Division of Anatomic Pathology and Histology, Catholic University School of Medicine "A. Gemelli," Rome, Italy; [6]Oral Pathology, Dublin Dental School and Hospital, University of Dublin Trinity College, Lincoln Place, Dublin, Ireland; [7]Department of Pathology, University of Dublin Trinity College, Trinity Centre for Health Sciences, St. James's Hospital, Dublin, Ireland; [8]Endocrinology Unit, Hospital "V. Cervello" of Palermo, Palermo, Italy; [9]Endocrinology Unit, Catholic University School of Medicine "A. Gemelli," Rome, Italy; [10]Department of Pathology, Brigham and Women's Hospital, Harvard Medical School; and [11]Department of Medicine, Brigham and Women's Hospital, Harvard Medical School, Boston, Massachusetts

Received 12/4/08; revised 2/10/09; accepted 3/3/09; published OnlineFirst 5/26/09. The costs of publication of this article were defrayed in part by the payment of page charges. This article must therefore be hereby marked *advertisement* in accordance with 18 U.S.C. Section 1734 solely to indicate this fact.

Note: Supplementary data for this article are available at Clinical Cancer Research Online (http://clincancerres.aacrjournals.org/).

Requests for reprints: Myles Brown, Department of Medical Oncology, Dana-Farber Cancer Institute, 44 Binney Street, D730, Boston, MA 02115. Phone: 617-632-3948; Fax: 617-582-8501; E-mail: myles_brown@dfci.harvard.edu.

doi:10.1158/1078-0432.CCR-08-3155

Translational Relevance

Anaplastic thyroid carcinoma (ATC) is highly aggressive and is responsible for more than half of thyroid carcinoma deaths, with a median survival of 3 to 6 months from diagnosis. Neither chemotherapy nor radiation therapy are effective in prolonging ATC patient survival; therefore, alternative systemic treatments for this cancer are urgently needed. *FOXA1* is a "pioneer transcription factor" overexpressed in some human cancers and involved in estrogen-dependent growth in breast cancer. We found *FOXA1* overexpression and gene copy number gain in >70% of ATC. In addition, we show that silencing of *FOXA1* leads to the growth arrest of ATC cell lines by reversing its inhibition of $p27^{kip1}$ transcription. These results suggest that *FOXA1* is a potential ATC oncogene and that therapies leading to the down-regulation of *FOXA1* could represent a novel therapeutic strategy. Development of *FOXA1*-directed therapies would be targeted to those tumors harboring *FOXA1* copy number gains at 14q21.1.

factor has been reported as amplified in lung and esophageal cancers (13) and also to be essential for estrogen signaling in breast cancer cells (14, 15). Indeed, *FOXA1* is required for estrogen receptor-α recruitment to chromatin, regulation of cyclin D1 expression, and cell cycle progression in breast cancer cells (16, 17). In addition, several other forkhead box subfamilies including FOXO, FOXM, FOXP, and FOXC have been linked to tumorigenesis and the progression of certain cancers, representing direct targets and indirect effectors of therapeutic intervention (18).

In this study, we have investigated *FOXA1* expression and copy number in endoderm-derived human thyroid tumors and its functional role in human thyroid carcinoma cell lines.

Materials and Methods

Antibodies

The following antibodies were used: β-actin (Sigma), lamin A/C (Cell Signaling Technology), FOXA1 (Ab5089 and Ab23738) for Western blot (Abcam), FOXA1 clone 2F83 for immunohistochemistry and Western blot (Seven Hills Bioreagents), $p27^{kip1}$ (Transduction Laboratories), cleaved poly(ADP-ribose) polymerase (Cell Signaling Technology), cyclin D1 (Thermo Scientific), MIB-1 (DAKO), p21 (BD Pharmingen), and cyclin E1 (Santa Cruz Biotechnology).

Human thyroid cell lines

The human thyroid carcinoma cell lines used in the study were BCPAP and TPC-1 (papillary thyroid carcinoma cell lines), WRO82-1 (follicular thyroid carcinoma cell line), and 8505c (undifferentiated thyroid carcinoma cell line). BCPAP were kindly provided by Dr. G. Damante (University of Udine) and WRO cell line was established by Dr. G.F. Juillard (University of California at Los Angeles) and provided by Dr. F. Frasca (University of Catania). TPC-1 cell line was kindly provided by Dr. F. Frasca. 8505c cell line (positive for cytokeratins, markers of epithelial tumors) was established by Dr. M. Akiyama (Radiation Effects Research Foundation). TE4 cell line (esophageal squamous adenocarcinoma) was provided by Dr. H. Ishii (Center for Molecular Medicine, Jichi Medical School). MCF-7 and MDA-231 (human breast cancer cell lines) were grown as in Eeckhoute et al. (19). All cell lines were grown in RPMI (BCPAP cells were grown in DMEM) supplemented with 10% FCS and ampicillin/streptomycin.

Cell transfections

For transfection assays, cells were grown in 60 mm well plates and transfected using Fugene-6 (Roche) in Opti-MEM for 48 h according to the manufacturer's instructions. Experiments were done at least three times in triplicate to ensure reproducibility of the results.

Short hairpin RNA

To stably suppress *FOXA1*, we used pLKO.1 lentiviral constructs containing two short hairpin RNA (shRNA) sequences generated by the RNAi Consortium, sh#1 anti-FOXA1 GCGTACTACCAAGGTGTGTAT and sh#2 anti-FOXA1 GCAGCATAAGCTGGACTTCAA. 8505c cells were also infected with the shRNA anti-GFP control. Lentiviral infections were done as follows. Briefly, 0.5×10^6 293T cells were seeded in 60 mm dishes and the day after cotransfected with pLKO.1 lentiviral constructs and packaging plasmids (gag-pol and VSV-G) using Fugene 6 (Roche). The medium containing the progeny virus released from the 293T cells was filtered by 0.45 μm filters, collected, and used to infect the 8505c cells for 3 to 6 h in the presence of 8 μg/mL polybrene (Sigma). The 8505c cells were incubated for additional 48 h, selected with puromycin (Sigma-Aldrich) for 48 h, and then lysed for Western blotting and real-time PCR analyses. *FOXA1* knockdown was confirmed by quantitative real-time PCR and Western blot. The experiments were done at least three times in triplicate to ensure reproducibility of the results.

Real-time PCR

RNA isolation and real-time reverse transcription-PCR were done as reported from Keeton and Brown (20). We used the following primers: GAAGATGGAAGGGCATGAAA and GCCTGAGTTCATGTTGCTGA for *FOXA1*, AATAAGGAAGCGACCTGCAA and ATTTGGGGAACCGTCTGAA for $p27^{kip1}$, CCGAAGTCAGTTCCTTGTGG and CATGGGTTCTGACGGACATC for $p21^{waf1}$, TGGAGGTCTGCGAGGAACAGAA and TGCAGGCGGCTCTTTTTCA for cyclin D1, and TACCCAAACTCAACGTGCAA and CATGATTTTCCAGACTTCCTCTC for cyclin E1. *FOXA1* mRNA expression was normalized to the 40 ribosomal protein S28. The presence of a single amplicon was systemically verified by dissociation curve analysis.

Nuclear and cytoplasmic fractionation

We used a lysis buffer composed of 1 mol/L HEPES, 5 mol/L NaCl, 1 mol/L $MgCl_2$, glycerol, Triton X-100, and 1 mol/L DTT. We scraped cells and washed twice in cold PBS, added 300 μL lysis buffer, and left the cells on ice 5 min, centrifuged the lysate at 2,800 rpm for 1 min at 4°C, and collected the supernatant (cytoplasmic fraction). We resuspended the pellet in 200 μL lysis buffer, added 28 μL of 5 mol/L NaCl, and mixed for 1 h at 4°C on a nutator, centrifuged the mixture at 14,000 rpm for 10 min at 4°C, and collected the supernatant (nuclear fraction).

Immunoblot analysis

Western blot assays were done as in Keeton and Brown (20). Bands were quantified by densitometry with the AlphaEase software (Alpha Innotec) according to the manufacturer's instructions.

Cell cycle analysis and bromodeoxyuridine assay

sh-control, sh#1-FOXA1, and sh#2-FOXA1 8505c cells were seeded at 2×10^3 per well in a six-well plate and grown. After 48 h, bromodeoxyuridine (BrdUrd; Upstate Cell Signaling Solutions) was added to a final concentration of 10 μmol/L for 1 h. 8505c cells were trypsinized and fixed in ethanol 75% prechilled (−20°C). The pelleted cells at 400 × *g* at room temperature were resuspended in PBS/0.5% bovine serum albumin (BSA), denatured in 2 mol/L HCl/0.5% BSA for

20 min at room temperature, washed with PBS/0.5% BSA, and centrifuged 5 min at 400 × *g* at room temperature. The cells were resuspended in 0.1 mol/L sodium borate (pH 8.5) for 2 min at room temperature, washed with PBS/0.5% BSA, centrifuged 5 min at 400 × *g* at room temperature, and resuspended in a solution PBS 0.5% Tween 20 containing FITC-conjugated anti-BrdUrd monoclonal antibody (BD Biosciences) according to the manufacturer's instructions and incubated in the dark for 30 min at 37°C. Finally, the cells were pelleted, washed twice with PBS/0.5% BSA, and resuspended in 500 μL of this solution. Propidium iodide was added to a final concentration of 10 μg/mL with RNase (10 mg/mL). Cells were incubated at room temperature for 30 min and then analyzed by flow cytometry on a FACSCalibur (Becton Dickinson Immunocytometry Systems) exciting at 488 nm and measuring the BrdUrd-FITC on the green fluorescence through a 514 nm bandpass filter and the DNA-linked red fluorescence (propidium iodide) through a 600 nm low pass filter, with compensation to reduce overlap between red and green fluorescence.

Apoptosis assay

Following 48 h sh-control, sh#1-FOXA1, and sh#2-FOXA1 8505c cells were collected and fixed overnight at 4°C with 75% ethanol for propidium iodide staining and flow cytometry analysis on a FACSCalibur to evaluate sub-G_1 cell populations. Proteins were extracted at the same time point and assayed for cleaved poly(ADP-ribose) polymerase expression by Western blot.

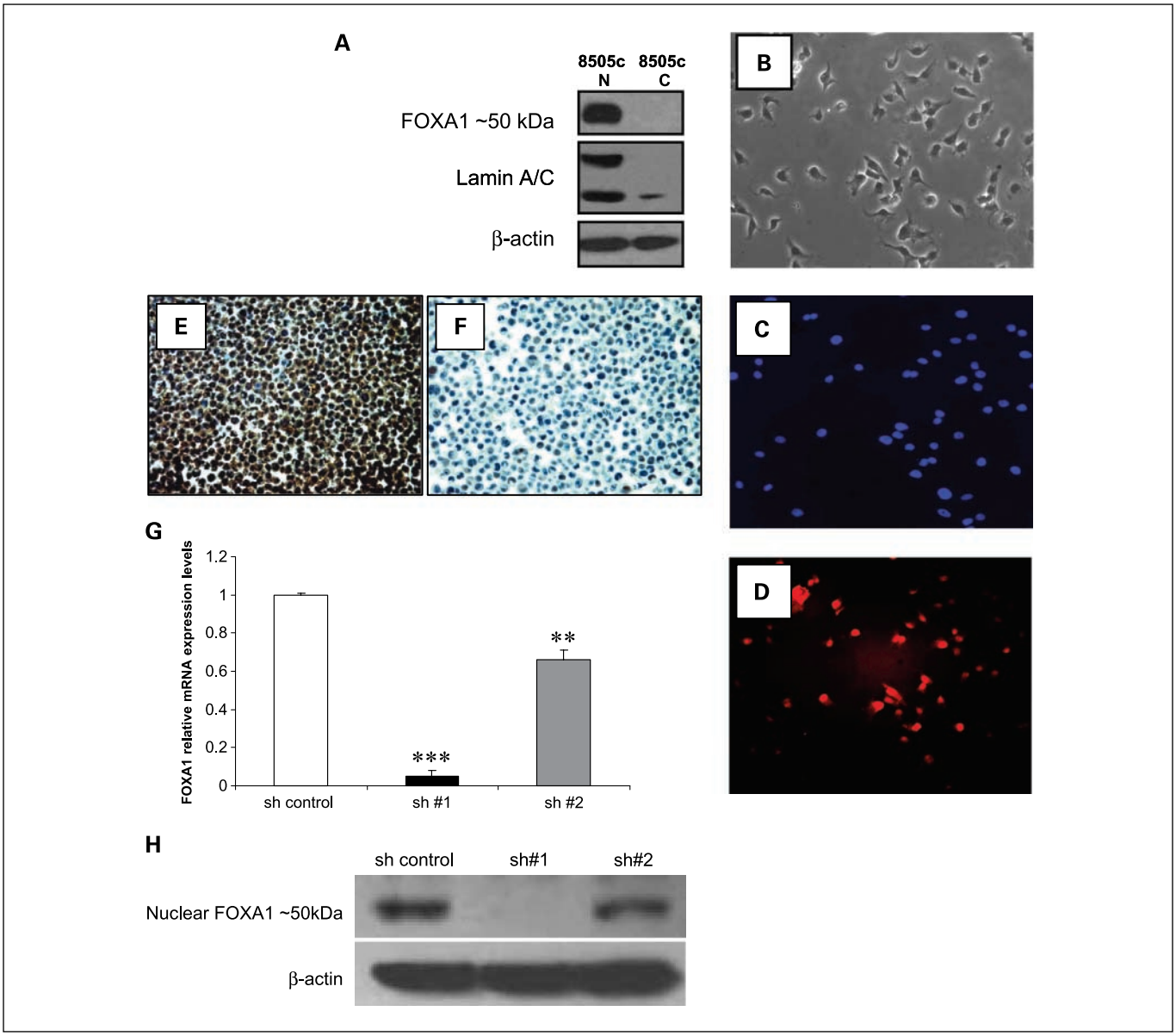

Fig. 1. FOXA1 expression in human thyroid carcinoma cells. FOXA1 is expressed in the nuclei (*N*) but not in the cytoplasm (*C*) of human undifferentiated thyroid carcinoma 8505c cells as confirmed by Western blot analysis (*A*) and immunofluorescence staining detected through Texas red-conjugated secondary antibody (magnification, ×20; *D*). *B,* bright-field image of 8505c cell monolayer. *C,* nuclear staining by 4′,6-diamidino-2-phenylindole. MCF-7 (*E*) and MDA-MB-231 (*F*) human breast cancer cells represented the positive and negative controls for FOXA1 immunostaining, respectively. *G, FOXA1* relative mRNA levels were significantly decreased in 8505c cells infected with sh#1 (average of the relative mRNA levels, 0.05 ± 0.03; ***, $P < 0.001$) and sh#2 (average of the relative mRNA levels, 0.66 ± 0.05; **, $P < 0.01$) versus control. *H,* 8505c cells were infected at the confluence of 60% for 3 to 6 h with two specific shRNAs anti-*FOXA1* (sh#1 and sh#2) or shRNA anti-GFP sequence (sh-control). Nuclear FOXA1 protein levels were completely depleted with sh#1 and decreased by ~30% with sh#2. Mean ± SD of at least three independent experiments.

Table 1. FOXA1 nuclear expression in human primary ATC

Case	Age	Gender	Histopathology	*FOXA1* localization	Positive nuclei*	FISH
1	64	M	ATC squamous	Nuclear	4	Gain/polysomy
2	58	F	ATC spindle cells	Nuclear	4	Gain/polysomy
3	51	F	ATC spindle cells	Nuclear	2	NR†
4	65	M	ATC osteoclastic like giant cells	Nuclear	2	NR
5	93	F	ATC spindle and giant cells	Nuclear	4	Disomy
6	80	M	ATC spindle cells	Nuclear	3	Gain/polysomy
7	68	M	ATC spindle and giant cells	Nuclear	4	Disomy
8	81	F	ATC spindle cells	Nuclear	4	Polysomy plus low-level gain of *FOXA1*
9	54	F	ATC + extensive PDTC + PTC foci	Nuclear	3	NR
10	65	F	ATC squamoid features	Nuclear	3	Gain/polysomy
11	68	M	ATC + PTC follicular variant foci	Nuclear	3	Polysomy plus low-level gain of *FOXA1*
12	52	M	ATC giant cells, rhabdoid differentiation + rhabdomyosarcomatous transformation	Nuclear	3	Gain/polysomy
13	70	F	ATC sarcomatoid variant, giant cells + PTC foci	Nuclear	4	Monosomy
14	77	M	ATC + focal PDTC + PTC foci	No	1	Gain/polysomy
15	43	M	ATC spindle cells	Nuclear	4	Gain/polysomy
16	43	M	ATC spindle cells	Nuclear	4	NR
17	74	F	ATC spindle cells, plasmacytoid and rhabdoid features	Nuclear	1	Monosomy
18	76	F	ATC osteoclastic like, giant cells + oncocytic PTC foci	Nuclear	2	Gain/polysomy
19	77	F	ATC + PTC foci	No	1	NR
20	87	F	ATC + PTC foci	Nuclear	2	NR

Abbreviations: PDTC, poorly differentiated thyroid carcinoma; PTC, papillary thyroid carcinoma; FTC, follicular thyroid carcinoma.
*Positive nuclei: 1, negative; 2, 1% to 10% of examined nuclei positive (low expression); 3, 11% to 50% of nuclei positive (high expression); and 4, >50% of nuclei positive (high expression).
†No results.

Paraffin-embedded thyroid tumors and tissue microarrays

Thyroid tumors were classified according to WHO diagnostic criteria (21). Tissue microarrays were composed from 177 cases: 15 normal thyroid tissues, 30 follicular adenomas, 58 nodular hyperplasia samples, 8 lymphocytic thyroiditis samples, 6 Graves, and 60 differentiated thyroid carcinomas: 48 papillary thyroid carcinomas (31 classic, 13 follicular variant, 3 microcarcinomas, and 1 oxyphilic variant), and 12 follicular thyroid carcinoma. Tissue microarrays were constructed according to previously established procedure (22) from anonymized archival blocks of formalin-fixed, paraffin-embedded tissue from the files of the Central Pathology Laboratory at St. James's Hospital, Dublin.

We studied 3 insular thyroid carcinomas and 20 ATC from 20 patients who underwent thyroidectomy (9 males and 11 females; average age, 67.3 ± 13.9 years; range, 43-93 years).

The ATC cases were screened for TTF-1, thyroglobulin, calcitonin, carcinoembryonic antigen, and cytokeratins. All the carcinomas displaying extensive immunoreactivity for calcitonin and/or carcinoembryonic antigen (medullary carcinoma) were not included in the series. Finally, all cases were reviewed by four pathologists (G.F., M.L., O.S., and V.N.).

An institutional review board protocol was approved by V.N. for the acquisition of paraffin-embedded thyroid tissue.

Cell pellet processing

After harvesting in PBS, human cancer cell lines were gently spun down (1,200 rpm for 5 min). The PBS was aspirated and the cells were resuspended in 4% paraformaldehyde for 15 min to fix them. Following a further PBS wash, the cells were then resuspended in 70% ethanol for 15 min. After aspiration of the ethanol, 2 mL of liquefied Histogel (Richard-Allan Scientific) were added to the cell pellet dropwise. The Histogel was gently vortexed and cooled on ice until solid. Histogel pellets were then processed in a tissue processor in the usual way.

Immunofluorescence

For immunofluorescence experiments, 5×10^4 cells were seeded in four-well chamber slides (BD Biosciences) for 24 h. Cells were washed twice with PBS, fixed with 4% paraformaldehyde for 10 min at room temperature, and permeabilized with PBS/0.1% Triton X-100 for 5 min at room temperature. After two washes with PBS, cells were blocked with PBS/1% BSA for 1 h followed by incubation with the primary antibody diluted in PBS/1% BSA for 1 h at room temperature. Cells were rinsed three times with PBS and then incubated with Texas red anti-mouse IgG (Vector Laboratories) for 1 h at room temperature, and the cells were washed three times. Finally, the chamber slides were stained with 4′,6-diamidino-2-phenylindole and mounted with Vectashield mounting medium (Vector Laboratories). Cells were imaged at ×20 with a Plan-Apochromat oil immersion lens on an Axioplan 2 Apoptome epifluorescence microscope (Zeiss).

Immunohistochemistry and scoring

Immunohistochemistry was done on 5 μm thick, formalin-fixed, paraffin-embedded tissue microarray and full sections using a primary antibody for *FOXA1*, $p27^{kip1}$, and MIB-1. The primary antibody was diluted 1:100 or 1:200 and incubated for 60 min at room temperature. Antigen retrieval was done for three successive 5 min microwave cycles in EDTA (pH 8). The BioGenex I 6000 autostainer was used for all subsequent steps (BioGenex). Primary antibody was detected using a biotin-avidin-conjugated secondary mouse antibody (1:200; Vector Laboratories), horseradish peroxidase and 3,3′-diaminobenzidine. Counterstaining was with hematoxylin.

Positive controls included human prostate tissues and MCF-7 cell pellets were run with each assay.

Nuclear staining for *FOXA1*, $p27^{kip1}$, and MIB-1 was assessed semiquantitatively by using the following scoring methods: (*a*) quantity: 1, negative; 2, 1% to 10% of examined nuclei positive (low expression); 3, 11% to 50% of nuclei positive; and 4, >50% of nuclei positive (high

expression). Scores were averaged across replicate cores. (*b*) Intensity: 0, negative; 1, weak; 2, moderate; and 3, strong.

Positively stained lymphocytes represented the internal control for $p27^{kip1}$ immunohistochemistry.

Cytogenetic analysis

Slide preparation. Sections (4 μm) of formalin-fixed, paraffin-embedded tumors were mounted on standard glass slides. Slides were baked at 60°C for at least 2 h and soaked for 15 min in xylene at 55°C and then in room temperature xylene for 15 min. Slides were dehydrated, air dried, boiled in 100 mmol/L Tris, 50 mmol/L EDTA (pH 7.0) for 1 h, and soaked in 2× SSC for 5 min. Slides were placed on a 37°C Thermobrite (StatSpin) and treated with Digest-All III solution (Invitrogen) for two 15 min digestions, fixed for 2 min in 10% phosphate-buffered formalin, and then dehydrated.

Fluorescence* in situ *hybridization. Each BAC DNA (1 μg) was labeled using a nick translation kit (Abbott Molecular/Vysis) following the manufacturer's directions. Labeled DNA was precipitated with 5 μL Cot-1 DNA (1 mg/mL stock) and resuspended in an appropriate volume of 50% Hybrisol (50% formamide, 2× SSC, 10% dextran sulfate). Slides and probes were denatured according to standard protocols. Hybridizations were done for at least 16 h at 37°C in a darkened humid chamber. Slides were washed in 2× SSC at 70°C for 10 min, rinsed 2× SSC at room temperature, and counterstained with 4′,6-diamidino-2-phenylindole II (Abbott Molecular/Vysis). Slides were imaged using an Olympus BX51 fluorescence microscope, and individual images were captured using an Applied Imaging system running CytoVision Genus version 3.9.

Probes-BAC clones RP11-314P15 (chromosome 14q12) and RP11-606C5 (spanning *FOXA1* at 14q21.1) were labeled with SpectrumGreen and SpectrumRed dUTP, respectively (Abbott Molecular/Vysis). Both BAC clones were obtained from the BAC-PAC Resource at Children's Hospital Oakland Research Institute.

Scoring. For each specimen, at least 50 tumor nuclei were scored for the number of signals corresponding to the *FOXA1* (T, test probe) and control probe (C), respectively, and T:C ratios were determined. Nuclei with a T:C ratio of 1:1 but with >2 signals per locus were scored as polysomic. Nuclei with a T:C ratio of >1 but with <3 signals per locus were scored as having *FOXA1* copy number gain. Nuclei with a T:C ratio >3 were scored as amplified for *FOXA1*.

Statistical analysis

Results were compared by Student's *t* test (*, $P < 0.05$; **, $P < 0.01$; ***, $P < 0.001$). FOXA1 and $p27^{kip1}$ protein expression levels were compared by Pearson correlation coefficient. Statistical analysis was carried out with Microsoft Excel software.

Results

FOXA1 *overexpression in ATC.* To investigate whether *FOXA1* is involved in thyroid tumorigenesis, we first examined *FOXA1* mRNA and protein expression levels in human thyroid cancer cell lines. Several of the commonly used human thyroid cell lines have been recently shown to be not only redundant (cross-contaminated) but also of nonthyroid origin likely arising from melanoma and primary human colon carcinoma (23). For this reason, we performed our experiments on those cells with confirmed authenticity (23).

We examined the expression of FOXA1 by Western blot (Fig. 1A) and immunofluorescence (Fig. 1B-D) in 8505c cells, an undifferentiated thyroid carcinoma cell line, WRO82-1 cells, a follicular carcinoma cell line, and BCPAP and TPC-1 cells, papillary carcinoma cell lines. Whereas WRO82-1, BCPAP, and TPC-1 were negative for FOXA1 expression (data not

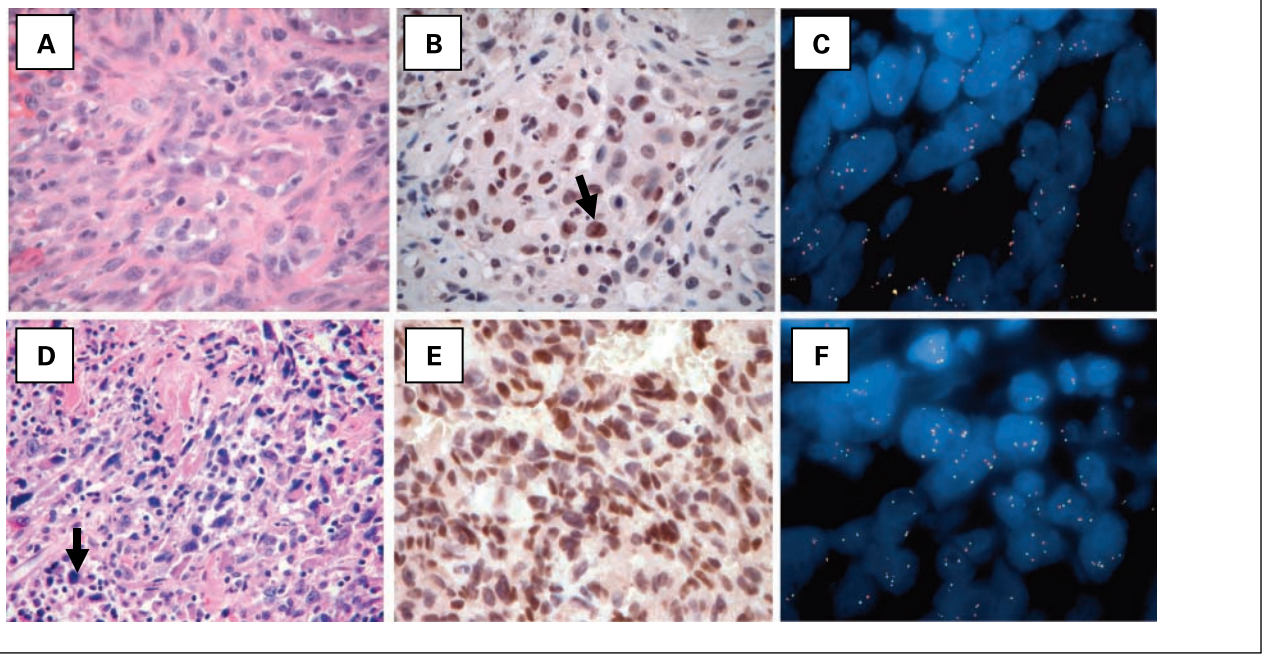

Fig. 2. FOXA1 expression in human primary thyroid undifferentiated carcinomas cells (ATC) and FISH analysis (all magnification, ×40). H&E stains of ATC cases showing squamoid morphology (*A*), classic giant cell and spindle cell morphology (*D*). *B* and *E*, intense nuclear FOXA1 expression in ATC cells by immunohistochemistry. Note the high mitotic activity (*arrows*). FOXA1 copy number gain by polysomy was observed in interphase tumor nuclei of ATC specimens (*C* and *F*) expressing high protein levels by immunohistochemistry (*B* and *E*). RP11-606C5 BAC clone (*red*) was cohybridized with a control RP11-314P15 BAC clone (*green*). *C* and *F*, representative sections from ATC with copy number gains of FOXA1. Intense FOXA1 nuclear staining is detected by immunohistochemical analysis (*B* and *E*).

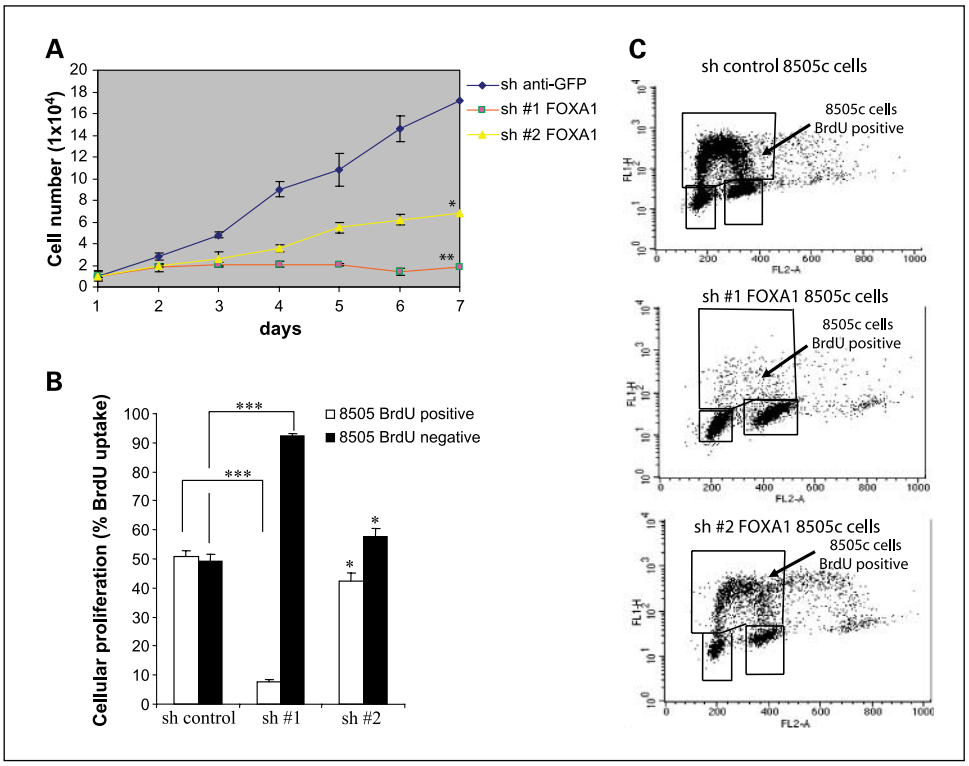

Fig. 3 Effects of *FOXA1* silencing on cell cycle of human thyroid carcinoma cells. 8505c cells were infected at the confluence of 60% for 3 to 6 h with two shRNAs against *FOXA1* (sh#1 and sh#2) or shRNA anti-GFP sequence (sh-control). *A,* 8505c cells infected with either sh#1 or sh#2 showed a significant decrease in cellular proliferation after 1 week (**, $P < 0.01$ and *, $P < 0.05$, respectively) versus control. *B* and *C,* similarly, BrdUrd incorporation (% of cell uptake) was dramatically decreased in 8505c cells infected with sh#1 *FOXA1* (7.4 ± 0.8%; **, $P < 0.001$), whereas a moderate decrease was detectable with sh#2 *FOXA1* (42.2 ± 2.8%; *, $P < 0.05$) versus control (49.2 ± 2.7%).

shown), 8505c cells expressed high levels of FOXA1, which was exclusive nuclear.

We confirmed the specificity of the anti-FOXA1 antibody by infecting 8505c cells with two lentiviral vectors expressing shRNAs specific for *FOXA1* (sh#1 and sh#2) or the control anti-GFP shRNA. *FOXA1* mRNA levels were decreased ~30% by sh#2 and by >90% by sh#1 (Fig. 1G). This degree of silencing of the *FOXA1* mRNA was reflected by a similar level of silencing of the protein (Fig. 1H), confirming both the specificity of the anti-FOXA1 antibody and the effectiveness of the shRNAs.

We next asked whether FOXA1 expression could be detected in primary ATC. Differentiated thyroid carcinomas and insular thyroid tumors were negative for FOXA1 as were normal thyroid tissue and benign lesions. Human ATC, which are characterized by marked cellular polymorphism (giant, spindle, and squamoid cells), eccentric nuclei, and conspicuous nucleoli, showed nuclear overexpression of FOXA1 protein (nuclear staining score 3 or 4; Table 1). FOXA1 was expressed diffusely within the tumors with moderate to strong intensity (overexpression) in 14 of 20 (70%) ATC cases (Fig. 2), whereas 4 of 20 (20%) showed focal and low expression and 2 of 20 (10%) were negative. Strong nuclear expression was mainly observed in ATC with squamoid or squamous growth pattern characterized by markedly atypical nuclei and high proliferative activity as shown by the presence of numerous atypical mitoses (Fig. 2) and high MIB-1 proliferative index (>85%; Supplementary Fig. S1A). Moreover, we found moderate to strong nuclear expression of FOXA1 in foci of squamous metaplasia of 2 cases of papillary thyroid cancer.

Finally, 7 ATC arising in association with small foci of differentiated papillary thyroid carcinoma showed FOXA1 expression only in the undifferentiated areas (Supplementary Fig. S1B). Differentiated papillary thyroid carcinomas areas showed a very weak nuclear and cytoplasmic expression barely above the threshold of detection and not comparable with the expression levels seen in ATC. These weakly expressing cases were considered negative for FOXA1 expression (Supplementary Fig. S1C).

Genomic gain of FOXA1 in human primary ATC specimens. To determine whether FOXA1 expression in ATC was linked to *FOXA1* copy number gain, we performed fluorescence *in situ* hybridization (FISH) analysis. FISH results were obtained for 14 of 20 ATC specimens because suboptimal tissue fixation precluded successful FISH analysis of six specimens. Hybridization of BAC RP11-606C5 to the TE4 cell line (human esophageal squamous carcinoma cell line with amplification of *FOXA1*) was used as positive control and confirmed a pattern of amplification consistent with a homogeneously staining region. A range of three to seven copies of *FOXA1* was detected in 10 of 14 (71.4%) ATC specimens (Fig. 2) and occurred as a result of polysomy (hybridization pattern consistent with multiple copies of chromosome 14). Disomy for *FOXA1* was observed for 2 of 14 (14%) ATC specimens, with a signal pattern consistent with monosomy 14 detected in the remaining 2 of 14 ATC specimens. In addition, 8 of 11 (72.7%) ATC tumors with nuclear FOXA1 protein overexpression showed copy number gain (Fig. 2), 2 of 11 (18.1%) specimens with overexpression were disomic for *FOXA1*, and 1 of 11 (9%) was consistent with monosomy 14 (Supplementary Fig. S2A). Two of 11 (18.1%) ATC with overexpressed *FOXA1* showed one to two additional copies in a subset (~22%) of tumor nuclei (Supplementary Fig. S2B). Finally, 8505c cells showed copy number gain of *FOXA1* due to polysomy (Supplementary Fig. S2C). In summary, we show that *FOXA1* is overexpressed and subject to copy number gain in human ATC.

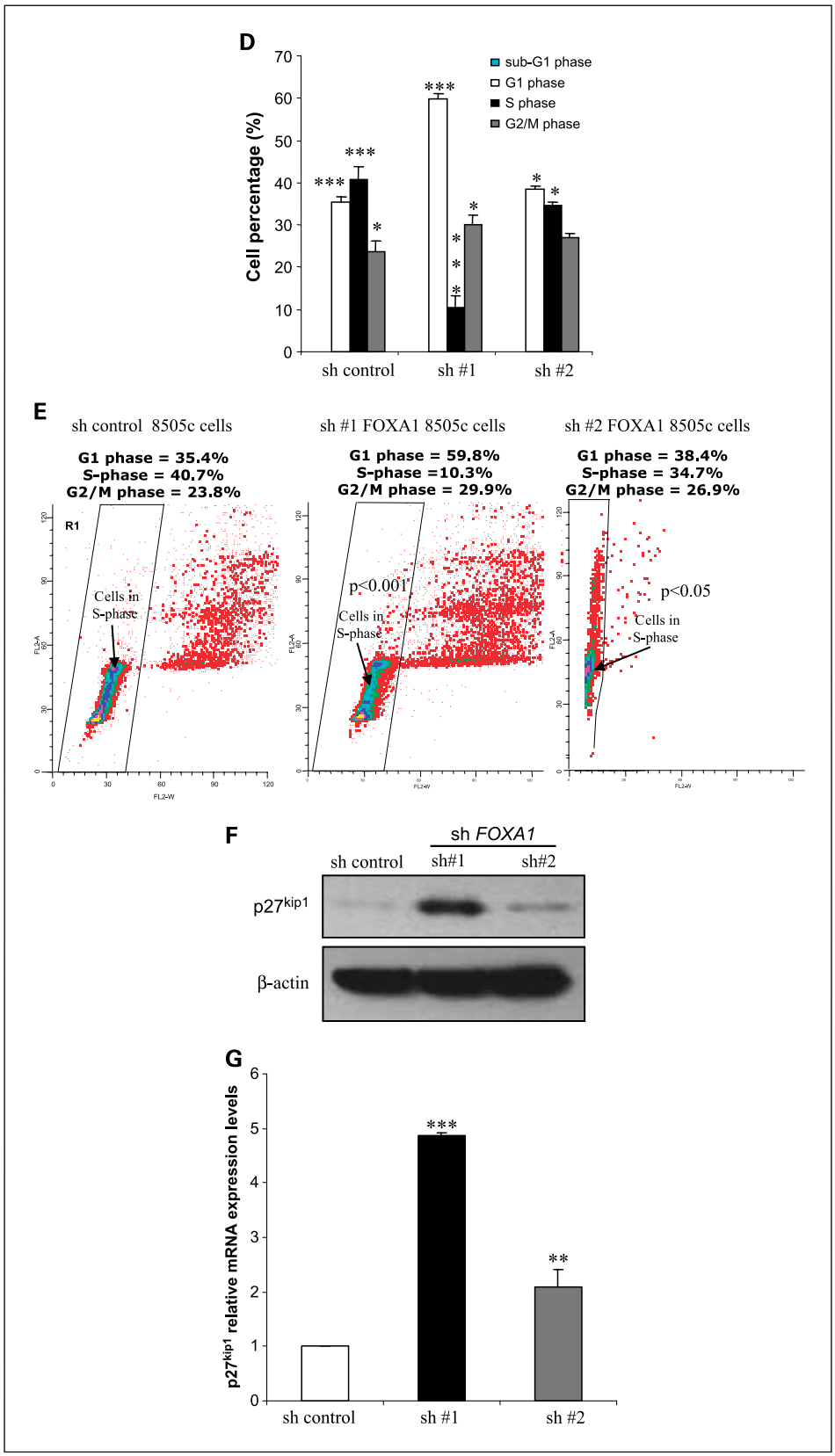

Fig. 3. *Continued. D* and *E,* cell cycle redistribution on treatment by *FOXA1* shRNAs. S-phase decrease was consistent with BrdUrd incorporation in 8505c cells infected with sh#1 (10.3 ± 3.0%; ***, $P < 0.001$) and sh#2 (34.7 ± 0.7%; *, $P < 0.05$) versus control (40.7 ± 2.9%). A growth arrest in G_1 phase but no apoptosis (sub-G_1 cell population) occurred on both sh#1 anti-*FOXA1* (58.8 ± 1.2%; ***, $P < 0.001$) and sh#2 (38.4 ± 0.7%; *, $P < 0.05$) versus control (35.4 ± 1.2%). Percentage of cells in G_2-M phase resulted also increased by sh#1 (29.9 ± 2.2%; *, $P < 0.05$). *F,* protein levels of cell cycle inhibitor $p27^{kip1}$ significantly increased in 8505c cells with both sh#1 (74.4%) and sh#2 (19.87%). *G,* $p27^{kip1}$ relative mRNA expression levels were also significantly rescued in sh#1 (average of the relative mRNA levels, 4.87 ± 0.04; ***, $P < 0.001$) and sh#2-infected 8505c cells (average of the relative mRNA levels, 2.1 ± 0.3; **, $P < 0.01$) versus control. Mean ± SD of at least three independent experiments.

Down-regulation of FOXA1 suppresses cell proliferation in human ATC cells correlated with transcriptional up-regulation of $p27^{kip1}$. We investigated the functional role of *FOXA1* in ATC cells by examining the effect of *FOXA1* silencing on cell cycle progression and cellular proliferation. Indeed, it has been previously shown that poorly or undifferentiated human thyroid cancer cells exhibit considerable imbalance of their cell cycle and multiple abnormal cell signal transduction pathways

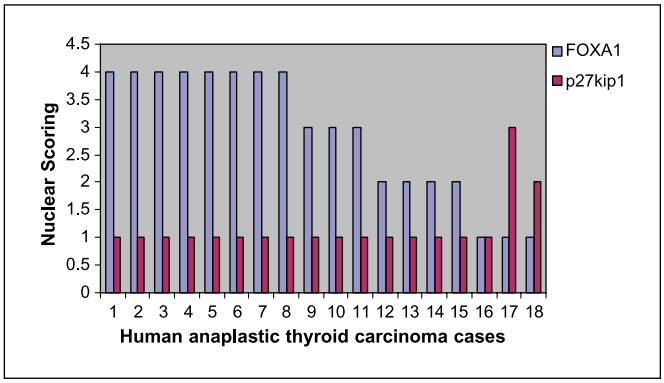

Fig. 4. Correlation between FOXA1 and $p27^{kip1}$ expression by immunohistochemical staining in human primary ATC. FOXA1 expression (mean % of positive nuclei) shows an inverse correlation ($r = -0.547$) with $p27^{kip1}$ expression (mean % of positive nuclei) in 18 human primary ATC. Nuclear scoring: no expression (1+), low expression (2+), and high expression (3 or 4+).

that determine rapid cellular proliferation, reduced apoptosis, and genomic instability (24).

To answer the question whether FOXA1 may affect cell proliferation, we conducted a cell cycle analysis in 8505c cells after *FOXA1* silencing by two independent shRNAs. Cell growth curves after 1 week of *FOXA1* showed a strong decrease of 8505c cellular proliferation by sh#1 ($P < 0.01$) and a slight decrease by sh#2 ($P < 0.05$; Fig. 3A), which were consistent with the levels of FOXA1 silencing (Fig. 1G-H). Similarly, BrdUrd incorporation (% of cell uptake) decreased in shRNA-treated cells compared with the control (sh#1 $P < 0.01$ and sh#2 $P < 0.05$; Fig. 3B and C).

We further investigated the cell cycle distribution of 8505c cells by flow cytometry analysis in which *FOXA1* had been silenced and observed a reduction of the fraction of cells in S phase (Fig. 3D and E), concomitant with an increase in the number of cells in both G_1 ($P < 0.001$) and G_2-M ($P < 0.05$) phases. The G_1-S transition of the cell cycle is controlled by different cyclins. Hence, we monitored the effect of *FOXA1* silencing on several of these molecular factors: $p21^{waf1}$, cyclin D1, and cyclin E1. None of these cyclins was differentially expressed between sh-*FOXA1* and sh-control in 8505c cells at either mRNA or protein level (Supplementary Fig. S3A and B).

However, we found that $p27^{kip1}$, a crucial cell cycle inhibitor, was significantly increased in 8505c cells infected with either *FOXA1* sh#1 or sh#2 at both mRNA and protein levels (Fig. 3F and G).

Finally, *FOXA1* silencing did not induce apoptosis in the infected cells as confirmed by flow cytometry analysis (absence of sub-G_1 cell population; Fig. 3D and E) and absence of cleaved poly (ADP-ribose) polymerase immunoblot (Supplementary Fig. S3B).

Inverse correlation between $p27^{kip1}$ and FOXA1 expression in human ATC specimens. $p27^{kip1}$ expression was investigated by immunohistochemistry in 20 human ATC cases. Two cases were excluded due to technical issues. The remaining 18 cases were divided into four categories with respect to $p27^{kip1}$ and FOXA1 expression and an inverse correlation between these protein levels was observed ($r = -0.547$; Fig. 4). Eleven (61%) of the cases had high nuclear *FOXA1* expression (3 or 4+) and absent $p27^{kip1}$ expression (1+; Fig. 4). Two (11%) of the cases had absent *FOXA1* expression (1+) and moderate to high $p27^{kip1}$ expression (2 or 3+; Fig. 4). Four (22%) of the cases had low *FOXA1* expression (2+) and absent $p27^{kip1}$ expression (1+; Fig. 4). One (6%) case had absent *FOXA1* and $p27^{kip1}$ expression (1+ for both; Fig. 4). In addition, 6 of 18 (33.3%) ATC showed a residual small focus of differentiated papillary thyroid carcinoma and weak $p27^{kip1}$ cytoplasmic expression was observed in all differentiated tumor foci associated with ATC (Supplementary Fig. S4).

Discussion

In this study, we found that human ATC express FOXA1 protein and show an intriguing link between FOXA1 expression, undifferentiated status, and cellular proliferation. Normal thyroid tissues, benign lesions, and differentiated thyroid carcinomas did not show detectable expression of FOXA1. Interestingly, we detected moderate nuclear protein levels of FOXA1 in squamous metaplasia foci of papillary well-differentiated thyroid carcinomas, a rare pathologic transformation that occurs in follicular thyroid tissues, still not well understood in terms of potential transition to undifferentiated thyroid cancer. This may suggest a role of FOXA1 in thyroid cell differentiation, because this transcription factor is already known to be expressed at 15.5 days in endoderm-derived mouse tissues including thyroid (25).

We found that FOXA1 nuclear overexpression was related to chromosome 14 gain in 72.7% of ATC. About 20% of the ATC that overexpressed FOXA1 showed low-level gain of *FOXA1* (1-2 additional copies), consistent with unbalanced rearrangements involving this locus. Our results are supported by previous studies showing copy number gain of other chromosomes in ATC (26–28) due to ploidy changes or unbalanced rearrangements that significantly occur in aggressive papillary thyroid carcinomas (29) and poorly differentiated thyroid cancers (30) and are less frequent in well-differentiated papillary thyroid carcinomas (26). This evidence suggests that copy number gains are genetic events of the progression from well-differentiated to poorly differentiated thyroid cancers to ATC, as they are also associated with an aggressive clinicopathologic behavior.

FOXA1 has been shown to be amplified and overexpressed in 6% to 9% of human esophageal and 40% lung adenocarcinomas (31, 32). A copy number gain due to polysomy of the *FOXA1* locus in ATC has not been reported. In our study, we found that 71.4% of ATC harbor this genomic alteration, supporting the idea that the genetic complexity of these tumors may play a role in producing the aggressive phenotype. We suggest that 14q gains are selected for because of *FOXA1* overexpression, although we cannot rule out the possibility that this is simply the result of genomic instability. Conversely, we found a low percentage of disomic ATC in the *FOXA1* locus, suggesting that other potential genetic alterations could occur. There was one ATC specimen (<10%) that showed *FOXA1* overexpression and monosomy of chromosome 14.

We showed that shRNA-mediated silencing of *FOXA1* significantly suppresses proliferation by blocking the G_1-S transition of anaplastic thyroid cancer cells. These data suggest that *FOXA1* might be one of the genes necessary and involved in the complex machinery of cellular proliferation of anaplastic thyroid cancer cells and could represent a potential new target for treatment of undifferentiated thyroid cancers. We

propose that inhibition of cell proliferation due to *FOXA1* silencing in undifferentiated thyroid carcinoma cells resulted in the reexpression of $p27^{kip1}$ mRNA and protein levels, which are usually very low or absent in this type of cancer. This is supported with the detection of an inverse correlation between loss of nuclear $p27^{kip1}$ protein and high levels of *FOXA1* protein in human ATC cells. Our results suggest that *FOXA1* in ATC cells could be a novel and important gene affecting cell proliferation by a potential transcriptional inhibition of $p27^{kip1}$. A *FOXA1* binding site within the BRCA1-responsive element of the $p27^{kip1}$ promoter has been identified (33). $p27^{kip1}$ has been widely known to be a critical inhibitor of cell cycle progression in human cancer cells (34), including thyroid cancer cells (35).

Cytoplasmic sequestration of $p27^{kip1}$ generally is associated with well-differentiated tumors, whereas loss of nuclear expression occurs in the aggressive tumoral phenotypes (36). $p27^{kip1}$ expression is controversial in ATC; in fact, some authors have described low protein levels (35, 36), whereas others have reported a similar quantity and intensity in ATC and differentiated thyroid carcinomas (37). Loss of nuclear $p27^{kip1}$ represents an independent predictor of metastatic disease in thyroid cancer (38) and in other human aggressive cancers associated with poor prognosis (39). Forkhead transcription factors such as FKHRL1 and FKHR are critical effectors of cell death and cell cycle arrest downstream of PTEN by $p27^{kip1}$ induction (40). Conversely, *FOXA1* may deregulate the inhibitor $p27^{kip1}$ in ATC cells and increase cell proliferation. Although different mechanisms are involved, FOXA1 is required for cellular proliferation in both undifferentiated thyroid carcinoma cells and breast cancer cells (16, 41–43). Indeed, FOXA1 silencing did not trigger a decrease in cyclin D1 levels in ATC as previously found in breast cancer (16). On the other hand, FOXA1 may stimulate ATC cell cycle progression through inhibition of $p27^{kip1}$ expression. This could be linked to direct and/or indirect cell type-specific activities of FOXA1 in the transcriptional regulation of these genes. Note that FOXA1 overexpression was able to induce $p27^{kip1}$ expression in breast cancer cell models (44), suggesting that mechanisms involved in cell growth regulation might depend on the amount of FOXA1 protein in different cell types.

Importantly, it has been recently shown that *FOXA1* regulates distinct transcriptional programs in cells of different lineages and translates epigenetic signatures into changes in chromatin structure, thereby establishing lineage-specific transcriptional enhancers and programs (45).

In summary, we show that (*a*) FOXA1 is expressed in human ATC, (*b*) increased FOXA1 expression is related to *FOXA1* gains and polysomy 14 in ATC, (*c*) *FOXA1* down-regulation by shRNA in ATC cells suppresses cell proliferation, and (*d*) *FOXA1* may be actively involved in cell proliferation and cell cycle regulation in ATC cells by regulating the expression of cell cycle inhibitor $p27^{kip1}$. Overall, our data reveal a novel potential role for FOXA1 as an oncogenic transcription factor in thyroid cancer. Therefore, identifying transcription factor networks involving *FOXA1* in ATC may offer new alternative treatments based on molecular targets.

Disclosure of Potential Conflicts of Interest

No potential conflicts of interest were disclosed.

Acknowledgments

C. Nucera is a recipient of a doctorate fellowship, Ph.D. program in Experimental Endocrinology and Metabolic Diseases (Endocrinology Unit, Department of Clinical-Experimental Medicine and Pharmacology, University of Messina).

We thank Natalie Vena and Eyoung Shin for technical support in FISH and immunohistochemistry experiments and Mathieu Lupien, Kirsten Fertuk, and Timothy Geistlinger for helpful suggestions.

References

1. Randolph GW, Daniels GH. Radioactive iodine lobe ablation as an alternative to completion thyroidectomy for follicular carcinoma of the thyroid. Thyroid 2002;12:989–96.
2. Nikiforov YE. Editorial. Anaplastic carcinoma of the thyroid. Will aurora B light a path for treatment? J Clin Endocrinol Metab 2005;90:1243–5.
3. Ain KB. Anaplastic thyroid carcinoma: a therapeutic challenge. Semin Surg Oncol 1999;16:64–9.
4. Cooper DS, Doherty GM, Haugen BR, et al.; The American Thyroid Association Guidelines Taskforce. Management guidelines for patients with thyroid nodules and differentiated thyroid cancer. Thyroid 2006;16:109–42.
5. Wreesmann VB, Ghossein RA, Patel SG, et al. Genome wide appraisal of thyroid cancer progression. Am J Pathol 2002;161:1549–56.
6. Wiseman SM, Griffith OL, Deen S, et al. Identification of molecular markers altered during transformation of differentiated into anaplastic thyroid carcinoma. Arch Surg 2007;142:717–27; discussion 727–9.
7. Nonaka D, Tang Y, Chiriboga L, Rivera M, Ghossein R. Diagnostic utility of thyroid transcription factors Pax8 and TTF-2 (FoxE1) in thyroid epithelial neoplasms. Mod Pathol 2008;21:192–200.
8. Friedman JR, Kaestner KH. The Foxa family of transcription factors in development and metabolism. Cell Mol Life Sci 2006;63:2317–28.
9. Lee CS, Friedman JR, Fulmer JT, Kaestner KH. The initiation of liver development is dependent on Foxa transcription factors. Nature 2005;435:944–7.
10. Besnard V, Wert SE, Hull WM, Whitsett JA. Immunohistochemical localization of Foxa1 and Foxa2 in mouse embryos and adult tissues. Gene Expr Patterns 2004;5:193–208.
11. Cirillo LA, Lin FR, Cuesta I, Friedman D, Jarnik M, Zaret KS. Opening of compacted chromatin by early developmental transcription factors HNF3 (FoxA) and GATA-4. Mol Cell 2002;9:279–89.
12. Gualdi R, Bossard P, Zheng M, Hamada Y, Coleman JR, Zaret KS. Hepatic specification of the gut endoderm *in vitro*: cell signaling and transcriptional control. Genes Dev 1996;10:1670–82.
13. Lin L, Miller CT, Contreras JI, et al. The hepatocyte nuclear factor 3α gene, HNF3α (FOXA1), on chromosome band 14q13 is amplified and overexpressed in esophageal and lung adenocarcinomas. Cancer Res 2002;62:5273–9.
14. Carroll JS, Brown M. Estrogen receptor target gene: an evolving concept. Mol Endocrinol 2006;20:1707–14.
15. Carroll JS, Meyer CA, Song J, et al. Genome-wide analysis of estrogen receptor binding sites. Nat Genet 2006;38:1289–97.
16. Eeckhoute J, Carroll JS, Geistlinger TR, Torres-Arzayus MI, Brown M. A cell-type-specific transcriptional network required for estrogen regulation of cyclin D1 and cell cycle progression in breast cancer. Genes Dev 2006;20:2513–26.
17. Carroll JS, Liu XS, Brodsky AS, et al. Chromosome-wide mapping of estrogen receptor binding reveals long-range regulation requiring the forkhead protein FoxA1. Cell 2005;122:33–43.
18. Myatt SS, Lam EW. The emerging roles of forkhead box (Fox) proteins in cancer. Nat Rev Cancer 2007;7:847–59.
19. Eeckhoute J, Keeton EK, Lupien M, Krum SA, Carroll JS, Brown M. Positive cross-regulatory loop ties GATA-3 to estrogen receptor α expression in breast cancer. Cancer Res 2007;67:6477–83.
20. Keeton EK, Brown M. Cell cycle progression stimulated by tamoxifen-bound estrogen receptor-α and promoter-specific effects in breast cancer cells deficient in N-CoR and SMRT. Mol Endocrinol 2005;19:1543–54.
21. Pathology and genetics of tumors of endocrine organs. In DeLellis RA, Lloyd RV, Heitz PU, Emg C, editors. Lyon: IARC Press; 2004.
22. Fedor HL, De Marzo AM. Practical methods for tissue microarray construction. Methods Mol Med 2005;103:89–101.
23. Schweppe RE, Klopper JP, Korch C, et al. DNA

profiling analysis of 40 human thyroid cancer cell lines reveals cross-contamination resulting in cell line redundancy and misidentification. J Clin Endocrinol Metab 2008;93:4331–41.

24. Wiseman SM, Masoudi H, Niblock P, et al. Anaplastic thyroid carcinoma: expression profile of targets for therapy offers new insights for disease treatment. Ann Surg Oncol 2007;14:719–29.

25. Besnard V, Wert SE, Hull WM, Whitsett JA. Immunohistochemical localization of Foxa1 and Foxa2 in mouse embryos and adult tissues. Gene Expr Patterns 2004;5:193–208.

26. Hemmer S, Wasenius VM, Knuutila S, Franssila K, Joensuu H. DNA copy number changes in thyroid carcinoma. Am J Pathol 1999;154:1539–47.

27. Miura D, Wada N, Chin K, et al. Anaplastic thyroid cancer: cytogenetic patterns by comparative genomic hybridization. Thyroid 2003;13:283–90.

28. Lee DH, Lee GK, Kong SY, et al. Epidermal growth factor receptor status in anaplastic thyroid carcinoma. J Clin Pathol 2007;60:881–4.

29. Kjellman P, Lagercrantz S, Höög A, Wallin G, Larsson C, Zedenius J. Gain of 1q and loss of 9q21.3-q32 are associated with a less favorable prognosis in papillary thyroid carcinoma. Genes Chromosomes Cancer 2001;32:43–9.

30. Wreesmann VB, Ghossein RA, Patel SG, et al. Genome-wide appraisal of thyroid cancer progression. Am J Pathol 2002;161:1549–56.

31. Lin L, Miller CT, Contreras JI, et al. The hepatocyte nuclear factor 3α gene, HNF3α (FOXA1), on chromosome band 14q13 is amplified and overexpressed in esophageal and lung adenocarcinomas. Cancer Res 2002;62:5273–9.

32. Yasui K, Imoto I, Fukuda Y, et al. Identification of target genes within an amplicon at 14q12-13 in esophageal squamous cell carcinoma. Genes Chromosomes Cancer 2001;32:112–8.

33. Williamson EA, Wolf I, O'Kelly J, Bose S, Tanosaki S, Koeffler HP. BRCA1 and FOXA1 proteins coregulate the expression of the cell cycle-dependent kinase inhibitor p27(Kip1). Oncogene 2006;25:1391–9.

34. Sicinski P, Zacharek S, Kim C. Duality of $p27^{Kip1}$ function in tumorigenesis. Genes Dev 2007;21:1703–6.

35. Baldassarre G, Belletti B, Bruni P, et al. Overexpressed cyclin D3 contributes to retaining the growth inhibitor p27 in the cytoplasm of thyroid tumor cells. J Clin Invest 1999;104:865–74.

36. Viglietto G, Motti ML, Fusco A. Understanding p27(kip1) deregulation in cancer: down-regulation or mislocalization. Cell Cycle 2002;1:394–400.

37. Erickson LA, Jin L, Wollan PC, Thompson GB, van Heerden J, Lloyd RV. Expression of $p27^{kip1}$ and Ki-67 in benign and malignant thyroid tumors. Mod Pathol 1998;11:169–74.

38. Kondo T, Ezzat S, Asa SL. Pathogenetic mechanisms in thyroid follicular-cell neoplasia. Nat Rev Cancer 2006;6:292–306.

39. Loda M, Cukor B, Tam SW, et al. Increased proteasome-dependent degradation of the cyclin-dependent kinase inhibitor p27 in aggressive colorectal carcinomas. Nat Med 1997;3:231–4.

40. Nakamura N, Ramaswamy S, Vazquez F, Signoretti S, Loda M, Sellers WR. Forkhead transcription factors are critical effectors of cell death and cell cycle arrest downstream of PTEN. Mol Cell Biol 2000;20:8969–82.

41. Laganière J, Deblois G, Lefebvre C, Bataille AR, Robert F, Giguère V. From the cover. Location analysis of estrogen receptor α target promoters reveals that FOXA1 defines a domain of the estrogen response. Proc Natl Acad Sci U S A 2005;102:11651–6.

42. Hua S, Kallen CB, Dhar R, et al. Genomic analysis of estrogen cascade reveals histone variant H2A Z associated with breast cancer progression. Mol Syst Biol 2008;4:188, Epub 2008 Apr 15.

43. Yamaguchi N, Ito E, Azuma S. FoxA1 as a lineage-specific oncogene in luminal type breast cancer. Biochem Biophys Res Commun 2008;365:711–7.

44. Wolf I, Bose S, Williamson EA, Miller CW, Karlan BY, Koeffler HP. FOXA1: growth inhibitor and a favorable prognostic factor in human breast cancer. Int J Cancer 2007;120:1013–22.

45. Lupien M, Eeckhoute J, Meyer CA, et al. FoxA1 translates epigenetic signatures into enhancer driven lineage-specific transcription. Cell 2008; 132:958–70.